

## A versatile synthetic route to the preparation of $^{15}\text{N}$ heterocycles

Nikita V. Chukanov,<sup>a,b</sup> Bryce M. Kidd,<sup>c</sup> Larisa M. Kovtunova,<sup>b,d</sup> Valerii I. Bukhtiyarov,<sup>d</sup>  
Roman V. Shchepin,<sup>e</sup> Eduard Y. Chekmenev,<sup>\*,e,g,h</sup> Boyd M. Goodson,<sup>c,f</sup> Kirill V.  
Kovtunov,<sup>\*,a,b</sup> Igor V. Koptug<sup>a,b</sup>

<sup>a</sup>International Tomography Center SB RAS, Novosibirsk, 630090, Russia

<sup>b</sup>Novosibirsk State University, Novosibirsk, 630090, Russia

<sup>c</sup>Department of Chemistry and Biochemistry, <sup>f</sup>Materials Technology Center, Southern Illinois University, Carbondale, IL 62901, USA

<sup>d</sup>Boreskov Institute of Catalysis SB RAS, Novosibirsk, 630090, Russia

<sup>e</sup>Department of Biomedical Engineering and Physics, Vanderbilt-Ingram Cancer Center (VICC), Vanderbilt Institute of Imaging Science (VUIIS), Department of Radiology, Vanderbilt University Medical Center, Nashville, TN 37232, USA

<sup>g</sup>Russian Academy of Sciences, Moscow, 119991, Russia

<sup>h</sup>Ibio, Department of Chemistry, Wayne State University, Karmanos Cancer Center, Detroit, MI 48083, USA

[\\*kovtunov@tomo.nsc.ru](mailto:*kovtunov@tomo.nsc.ru)

[\\*chekmenev@wayne.edu](mailto:*chekmenev@wayne.edu)

KEYWORDS: Parahydrogen; PHIP; Hyperpolarization; Contrast Agent; pyridine;  $^{15}\text{N}$ ; MRI

This article has been accepted for publication and undergone full peer review but has not been through the copyediting, typesetting, pagination and proofreading process which may lead to differences between this version and the Version of Record. Please cite this article as doi: 10.1002/jlcr.3699

## Abstract

A robust medium-scale (~3 g) synthetic method for  $^{15}\text{N}$  labeling of pyridine ( $^{15}\text{N}$ -Py) is reported based on the Zincke reaction.  $^{15}\text{N}$  enrichment in excess of 81% was achieved with ~33% yield.  $^{15}\text{N}$ -Py serves as a standard substrate in a wide range of studies employing a hyperpolarization technique for efficient polarization transfer from parahydrogen to heteronuclei; this technique, called SABRE (Signal Amplification by Reversible Exchange), employs a simultaneous chemical exchange of parahydrogen and to-be-hyperpolarized substrate (e.g. pyridine) on metal centers. In studies aimed at the development of hyperpolarized contrast agents for *in vivo* molecular imaging, pyridine is often employed either as a model substrate (for hyperpolarization technique development, quality assurance, and phantom imaging studies) or as a co-substrate to facilitate more efficient hyperpolarization of a wide range of emerging contrast agents (e.g. nicotinamide). Here, the produced  $^{15}\text{N}$ -Py was used for the feasibility study of spontaneous  $^{15}\text{N}$  hyperpolarization at high magnetic (HF) fields (7 T and 9.4 T) of an NMR spectrometer and a MRI scanner, respectively. SABRE hyperpolarization enabled acquisition of 2D MRI imaging of catalyst-bound  $^{15}\text{N}$ -pyridine with  $75\times 75\text{ mm}^2$  field of view (FOV),  $32\times 32$  matrix size, demonstrating the feasibility of  $^{15}\text{N}$  HF-SABRE molecular imaging with  $2.4\times 2.4\text{ mm}^2$  spatial resolution.

## Introduction

Isotopic labelling with stable isotopes of hydrogen, carbon, oxygen, and nitrogen is increasingly used in a wide range of applications.<sup>[1-4]</sup>  $^{13}\text{C}$  and  $^{15}\text{N}$  labels have also been recently employed for synthesis of a wide range of biomolecules with an eye towards magnetic resonance applications.<sup>[2]</sup> Indeed, for such applications NMR hyperpolarization techniques are often employed to generate non-equilibrium nuclear spin polarization (typically  $\sim 10^{-6}$ /Tesla at room temperature) all the way to near unity (or 100%) nuclear spin polarization.<sup>[5-8]</sup> The process of hyperpolarization (*i.e.*, significant polarization enhancement above the thermal polarization level induced by the applied static magnetic field) results in corresponding gains (by several orders of magnitude) of NMR signals. These hyperpolarized (HP) biomolecules can be employed as contrast agents for *in vivo* studies, which opens up new opportunities for probing metabolism non-invasively by means of HP MRI.<sup>[9, 10]</sup>

Despite the MRI signal boost provided by hyperpolarization, biomedical applications of HP contrast agents are often limited<sup>[2, 11]</sup> when isotopic labeling is not employed due to low natural abundance of key biologically relevant spin- $\frac{1}{2}$  nuclei: e.g.  $^{13}\text{C}$  (1.1%) and  $^{15}\text{N}$  (0.37%). Therefore,  $^{13}\text{C}$  and  $^{15}\text{N}$  labeling is required to enhance the MRI signals in the context of biomedical applications, which are presently the main drivers behind the development of hyperpolarization techniques in general.<sup>[2, 9, 12]</sup>

Although proton spins have a higher detection sensitivity (compared to that of  $^{13}\text{C}$  and  $^{15}\text{N}$  nuclei) and are very abundant (near 100%) in the context of MRI applications, they are rarely employed for hyperpolarization of HP contrast agents owing to their relatively short spin-lattice relaxation time constant ( $T_1$ ) values (typically in the range of a few seconds). As a result, proton-based HP contrast agents<sup>[13, 14]</sup> undergo very rapid depolarization.<sup>[15-22]</sup> For example, HP contrast agent loses  $\sim 95\%$  of its initial polarization level (and effective potency) within  $3 \times T_1$ .  $^{13}\text{C}$  and  $^{15}\text{N}$  nuclear spins of biomolecules have  $T_1$  values of the order of tens of seconds<sup>[2, 23-30]</sup> and several minutes<sup>[31, 32]</sup> (*in vivo*) respectively. Therefore, HP  $^{13}\text{C}$  and  $^{15}\text{N}$  sites provide more efficient means of polarization storage in the context of preparation, administration, and MRI imaging of HP contrast agents.<sup>[9, 33-40]</sup> Additionally,  $^{13}\text{C}$  and  $^{15}\text{N}$  HP contrast agents do not suffer from competition with any significant *in vivo* background signal, compared to the large water and lipid background signals in HP proton MRI.<sup>[11, 41-43]</sup>

Historically  $^{13}\text{C}$ -based HP contrast agents have been introduced first, due to more readily available  $^{13}\text{C}$ -enriched compounds and efficient hyperpolarization processes using dissolution Dynamic Nuclear Polarization (d-DNP)<sup>[44]</sup> in the context of  $^{13}\text{C}$  hyperpolarization

of carboxyl groups in a wide range of biomolecules.<sup>[2]</sup> Isolated  $^{13}\text{C}$  carboxyl groups (i.e. without directly attached protons, which typically decrease  $T_1$  of neighboring  $^{13}\text{C}$  and  $^{15}\text{N}$  sites) demonstrate relatively long *in vivo*  $T_1$  values for HP contrast agents, often approaching ~1 minute.<sup>[2]</sup>

Nevertheless,  $^{15}\text{N}$  HP contrast agents have significantly longer  $T_1$  values of more than 2 minutes<sup>[31]</sup> *in vivo*. A number of HP compounds exhibit *in vitro*  $^{15}\text{N}$   $T_1$  values on the order of 3-10 minutes.<sup>[33, 38, 45]</sup> Moreover, the use of long-lived spin states<sup>[46]</sup> offer an intriguing possibility of extending the exponential decay constant to 20+ minutes for  $^{15}\text{N}$  sites.<sup>[40]</sup> Furthermore,  $^{15}\text{N}$  has a significantly greater (by at least several fold) chemical shift dispersion compared to that of  $^{13}\text{C}$ , in part because many relevant N-containing species possess lone pairs on the nitrogen site; therefore, HP  $^{15}\text{N}$  sites can serve as molecular probes for sensing characteristics of the local environment<sup>[37]</sup> such as pH.<sup>[43, 47]</sup>

Technical improvements of the d-DNP technique have recently allowed for more efficient hyperpolarization of  $^{15}\text{N}$  sites.<sup>[43]</sup> Additionally, a second method for the HP contrast agent production based on parahydrogen (a spin isomer of hydrogen) called Signal Amplification By Reversible Exchange (SABRE)<sup>[48, 49]</sup> has been shown to be very efficient for hyperpolarization of  $^{15}\text{N}$  sites in a number of molecular frameworks, including those found in several biomolecules.<sup>[47, 50-55]</sup> A variant of SABRE, dubbed “SABRE-SHEATH” (SABRE in SHield Enables Alignment Transfer to Heteronuclei)<sup>[56, 57]</sup> can produce  $^{15}\text{N}$  polarization ( $\%P_{^{15}\text{N}}$ ) in excess of 20% in less than 1 minute.<sup>[52]</sup> Moreover unlike the case with d-DNP, which requires expensive cryogenic and magnetic equipment, SABRE-SHEATH is technologically undemanding, and therefore it is a relatively cheap hyperpolarization technique.<sup>[53]</sup> As a result of these recent developments in d-DNP and  $^{15}\text{N}$  SABRE-SHEATH, the interest for use of HP  $^{15}\text{N}$  labeled biomolecules has been rekindled.<sup>[38, 58-61]</sup>

Regardless of the technique employed (d-DNP or SABRE), the structure of a given synthesized  $^{15}\text{N}$ -labeled compound is not altered during the hyperpolarization process. The reader is directed to other review papers on d-DNP hyperpolarization,<sup>[2, 8, 62]</sup> which is outside the scope of this work. In the SABRE approach, the to-be-hyperpolarized substrate and parahydrogen ( $\text{pH}_2$ ) exchange reversibly with a metal complex (Figure 1).<sup>[63]</sup> The first observation of the SABRE effect was realized for pyridine and in subsequent years it was extended to many N-<sup>[40, 48, 52, 53, 63, 64]</sup> and S-<sup>[65]</sup> containing heterocycles and other N-based functional groups.<sup>[40]</sup> Importantly, the SABRE approach allows the transfer of spin order not only to the protons of the corresponding substrates but also to the heteronuclei; to achieve

that step, pulse sequences<sup>[66, 67]</sup> or a magnetic shield<sup>[68]</sup> (SABRE-SHEATH)<sup>[56, 57]</sup> can be successfully applied. Moreover, while SABRE-SHEATH (the most efficient technique in terms of both speed of polarization and maximum demonstrated % $P_{15N}$ <sup>[52]</sup>) has also been shown to successfully hyperpolarize  $^{13}C$ <sup>[69, 70]</sup> and  $^{19}F$ <sup>[71]</sup> sites (and potentially other spin  $\frac{1}{2}$  nuclei<sup>[72]</sup>) in biomolecular frameworks, it has been recognized that the presence of a spin  $\frac{1}{2}$   $^{15}N$  at the site for catalyst binding<sup>[69]</sup> (i.e., the N atom directly participating in exchangeable binding to the metal center, Figure 1) enables significantly more efficient polarization of  $^{13}C$  and other biologically relevant sites. To summarize,  $^{15}N$ -labeling is critical for both  $^{15}N$ -based HP contrast agents as well as other ( $^{13}C$ ,  $^{19}F$ , etc.-based) HP contrast agents in the context of the SABRE-SHEATH hyperpolarization technique.

### $^{15}N$ SABRE-SHEATH hyperpolarization

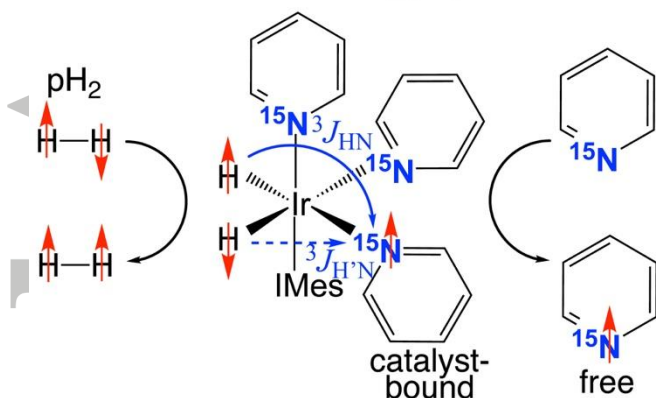


**Figure 1.** A schematic diagram of Signal Amplification by Reversible Exchange (SABRE)<sup>[48, 49, 73, 74]</sup> for the case of efficient hyperpolarization of the  $^{15}N$  site of  $^{15}N$ -pyridine using the SABRE-SHEATH approach. Note the simultaneous chemical exchange of  $pD_2$  and the to-be-hyperpolarized substrate (here,  $^{15}N$ -pyridine) in the equatorial positions of this IrIMes hexacoordinate complex<sup>[75]</sup> and the spontaneous nature of polarization transfer via two-bond spin-spin couplings when the process is performed at the matching magnetic field of approximately 1 micro-Tesla ( $\mu T$ ).<sup>[56, 57, 76]</sup>

Recently, SABRE-SHEATH has been employed to hyperpolarize several  $^{15}N$ -enriched molecules:  $^{15}N$ -pyridine,<sup>[56]</sup>  $^{15}N_2$ -imidazole,<sup>[47, 59]</sup>  $^{15}N$ -nicotinamide,<sup>[56, 58]</sup> etc. Most of these compounds in the  $^{15}N$ -labeled form are not available commercially or available at a very high (>\$500/0.1 g) cost not very well suitable for the development of biomedical applications on a human scale requiring  $\sim 1$  g of HP contrast agent.<sup>[9]</sup> Robust synthetic approaches are certainly required to enable this field of molecular imaging with a broad range of  $^{15}N$ -labeled biomolecules.

There are two major synthetic approaches/strategies for preparation of  $^{15}\text{N}$ -labeled heterocycles. The first one is *de novo*, i.e. from Latin “from scratch”, when the desired molecular framework is built using reagents (components) that are smaller than and different from the target product. We have recently demonstrated this approach in the context of  $^{15}\text{N}$  SABRE-SHEATH for preparation of  $^{15}\text{N}_2$ -imidazole.<sup>[59]</sup> The second strategy employs the target contrast agent itself without  $^{15}\text{N}$  enrichment as a starting material, where the  $^{14}\text{N}$ -site (natural abundance of nitrogen isotopes) is effectively “replaced” by the  $^{15}\text{N}$  isotope. While both approaches have their merits, the second approach is attractive because a number of complex biomolecules (including drugs) can be potentially enriched in just two steps. For example, we have recently demonstrated this approach using a Zincke salt<sup>[77]</sup> on  $^{15}\text{N}$ -nicotinamide, and demonstrated good yields along with ~98%  $^{15}\text{N}$  enrichment.<sup>[58]</sup>

The work presented here focuses on the synthesis of  $^{15}\text{N}$ -Py using the Zincke<sup>[77]</sup> reaction.  $^{15}\text{N}$ -Py is an important molecular target in itself, because it is one of the most studied molecule by SABRE hyperpolarization methods in general, and therefore, it can be useful for mechanistic and phantom imaging studies.<sup>[67, 69, 78-82]</sup> Moreover, a variant of the SABRE-SHEATH approach has been demonstrated where Py is added to enhance polarization of other HP substrates (e.g.  $^{15}\text{N}$ -nicotinamide,<sup>[58]</sup> and  $^{15}\text{N}$ -acetonitrile<sup>[69]</sup>), indicating that  $^{15}\text{N}$ -Py-mediated SABRE catalyst activation could be useful for preparation of other HP contrast agents via SABRE-SHEATH. More importantly,  $^{15}\text{N}$ -Py embodies a molecular framework around which many other useful  $^{15}\text{N}$  HP contrast agents could be developed in the future in the form of the substituted  $^{15}\text{N}$ -pyridines (which is an active and on-going effort of our collaboration). While other synthetic approach for preparation of  $^{15}\text{N}$ -pyridine has been reported,<sup>[83]</sup> it lacks versatility for preparation of substituted  $^{15}\text{N}$ -pyridine-based biomolecules, e.g. nicotinamide, etc., which is of significant interest to hyperpolarized MR community.<sup>[84]</sup> Therefore, the synthetic approach studied here would be of significant interest for future synthetic efforts in this field. We note that the starting material of the approach demonstrated here is relatively inexpensive  $^{15}\text{NH}_4\text{Cl}$  (<\$20/g ca. 2017), and the product was produced with ~33% yield and >81%  $^{15}\text{N}$  enrichment, showing an efficient route for  $^{15}\text{N}$  enrichment of pyridine-based (and potentially other) heterocycles. Finally, the demonstrated labeled  $^{15}\text{N}$ -Py and potentially other  $^{15}\text{N}$ -labeled compounds enabled by this approach can be hyperpolarized by both SABRE and d-DNP hyperpolarization techniques, and therefore, a broad community of those working in the field of HP molecular imaging would benefit from the work described here.

Here in particular, we have employed the prepared  $^{15}\text{N}$ -Py material for the feasibility study of spontaneous  $^{15}\text{N}$  hyperpolarization and  $^{15}\text{N}$  molecular imaging at high magnetic field<sup>[85]</sup> of a 9.4 T MRI scanner and a 7.0 T NMR spectrometer.

## Experimental

### *General*

All solvents were purchased from common vendors and were used as received. All NMR spectra and images ( $^1\text{H}$ ,  $^{13}\text{C}$ ,  $^{15}\text{N}$ ) were recorded on Bruker 300 MHz and Bruker 400 MHz Avance III NMR spectrometers. 1-chloro-2,4-dinitrobenzene was recrystallized from ethanol. N-(2,4-Dinitrophenyl) pyridinium chloride was prepared by interaction of pyridine with 1-chloro-2,4-dinitrobenzene in acetone according to a procedure similar to that reported previously.<sup>[86]</sup>

### *Synthesis of $^{15}\text{N}$ -Pyridine*

First (small-scale) procedure. 150 mL of anhydrous methanol at 0 °C was placed in a round bottom flask. Next sodium metal (0.43 g, 18.7 mmol) was added with continuous stirring. As soon as the sodium has completely reacted (no hydrogen gas observed),  $^{15}\text{NH}_4\text{Cl}$  (1.00 g, 18.35 mmol) was added. Next, (i) a solution of N-(2,4-Dinitrophenyl) pyridinium chloride (2.63 g, 9.34 mmol) in anhydrous methanol (20 mL) was added drop-by-drop to the mixture under stirring and the mixture was stirred for one week at room temperature, and (ii) activated carbon (2.00 g) was added and stirred for 30 minutes and then was filtered. The supernatant solution was distilled, and a concentrated hydrochloric acid (8 mL) was added to the distillate, and the resulting solution was evaporated to dryness under vacuum. The formed pyridinium hydrochloride was placed in 2 mL flask using a minimal amount of water for the quantitative collection of the formed hydrochloride, and excess of sodium hydroxide (1.5 g) was then added. The mixture was cooled down by liquid nitrogen during neutralization, and the reaction was deemed completed. The resulting mixture was distilled, and  $^{15}\text{N}$ -Py was obtained as an aqueous solution (0.64 g) with concentration of about 25% ( $^{15}\text{N}$  isotopic purity is better than 60%), and the produced material was used in the subsequent NMR/MRI experiments. The total yield of pyridine was about 22%.

Second (medium-scale optimized) procedure. Pyridine (60.00 mL, 744 mmol) and 2,4-dinitro-chlorobenzene (25.4 g, 125 mmol) were placed in an oven-dried round bottom flask (1 L) supplied with a magnetic stir bar. The solids were dissolved in anhydrous methanol and

left to stir at room temperature for 2 days under inert (argon) atmosphere. The flask was placed on a rotary evaporator to remove excess of unreacted pyridine, and anhydrous THF (300 mL) was added to the reaction mixture. White amorphous residue was formed on the bottom of the flask. THF was decanted carefully, leaving the residue on the bottom of the flask. Another portion of anhydrous THF (100 mL) was added rapidly, and the flask was rotated several times and left for several minutes before THF was carefully decanted from the residue. The THF wash was repeated 5 times. The flask was placed on a rotary evaporator to remove last traces of THF from the pyridine-Zincke salt. Anhydrous methanol (150 mL) was added, and the flask was flashed with argon and put aside.

To an oven-dried round bottom flask (5 L) supplied with a stir bar,  $^{15}\text{NH}_4\text{Cl}$  (574 mmol, 31.26 g) and anhydrous methanol (3 L) were added. The solution was cooled to 0 °C and sodium methoxide methanolic solution (30 wt%, 516 mmol, 118 mL) was added drop-wise. The methanolic solution of pyridine-Zincke salt (described above) was added dropwise to the flask. The resulting solution was left to stir under an inert atmosphere (argon) for 2 days. The supernatant solution was distilled, and 2 M solution of hydrochloric acid (250 mL) in  $\text{Et}_2\text{O}$  was added to the distillate (pH ~ 2), and the resulting solution was evaporated to dryness under vacuum. The resulting crude pyridine hydrochloride was placed in 100 mL flask, and an excess of solid sodium hydroxide (25 g) was added and the mixture was distilled. Molecular sieves (4 Å, 5.7 g, Fisher chemical, P/N M514-500) were added to the obtained  $^{15}\text{N}$ -Py. A second distillation and drying by molecular sieves allowed the preparation of 3.3 g of  $^{15}\text{N}$ -Py (yield: 33%;  $^{15}\text{N}$  isotopic purity is >81%), Figure 2.

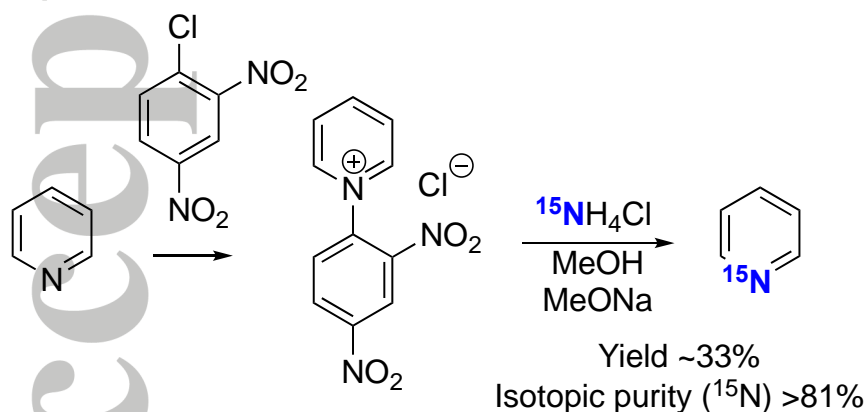


**Figure 2.** The overall scheme of  $^{15}\text{N}$ -Py enrichment with  $^{15}\text{N}$  (from  $^{15}\text{NH}_4\text{Cl}$  source) via Zincke salt formation.

### Parahydrogen preparation, NMR and MRI experiments

Enrichment of parahydrogen ( $pH_2$ ) spin isomer was performed with a Bruker parahydrogen generator, that allows filling of a 0.9 L-tank with 7 atm of  $\sim 90\%$   $pH_2$  in approximately 100 minutes.

For the observation of  $^{15}N$  enhanced resonances the polarization transfer from  $pH_2$ -derived protons to  $^{15}N$  nuclei of  $^{15}N$ -Py (prepared via the first procedure described above) was realized via high-field SABRE (HF-SABRE) and SABRE-SHEATH approaches. Specifically,  $pH_2$  gas was bubbled (flow rate  $30 \text{ mL}\cdot\text{min}^{-1}$ ) through a 1/16 in. (OD) Teflon capillary extended to the bottom of a 5 mm medium-wall NMR tube containing a SABRE catalyst solution and  $^{15}N$ -Py (10 mM of  $\text{IrCl}(\text{COD})(\text{IMes})$  ( $\text{IMes} = 1,3\text{-bis}(2,4,6\text{-trimethylphenyl})\text{imidazol-2-ylidene}$ ,<sup>[75, 87]</sup> COD = cyclooctadiene; note this catalyst precursor was synthesized in accord with a previously reported procedure<sup>[85]</sup>) in  $\text{CD}_3\text{OD}$ .  $pH_2$  bubbling occurred in the magnetic shield for the SABRE-SHEATH approach. When the gas flow was halted, the sample was transferred to the high magnetic field, where  $^{15}N$  NMR spectra were recorded. For the HF-SABRE method  $pH_2$  bubbling was performed at high magnetic field (7 T) of NMR spectrometer during the detection of  $^{15}N$  resonances.

The MRI investigations were carried out with a 400 MHz Bruker scanner equipped with a  $^{15}N/^1H$  25 mm MRI probe. The standard EPI (echo-planar imaging) MRI pulse sequence was utilized with  $32\times 32$  matrix size, 4 averages, 11 ms echo time (TE),  $75\times 75\text{mm}^2$  field of view (FOV), and approximately 4 seconds' total scan time. The MRI experiments were performed using a 10-mm outer diameter NMR tube.

### Results and Discussion

To the best of our knowledge, there is only one method for the synthesis of  $^{15}N$ -Py: the reaction of 2-ethoxy-3,4-dihydro-2*H*-pyran with  $^{15}N\text{-NH}_4\text{Cl}$  in the presence of methylene blue (Figure 3).<sup>[83]</sup> The yield was reported as 55% when the equivalent ratio of pyran derivative and  $^{15}N\text{NH}_4\text{Cl}$  was used. In a similar manner, 4-methylpyridine was obtained from 2-ethoxy-4-methyl-3,4-dihydro-2*H*-pyran.<sup>[86]</sup> The main limitation of this synthetic approach is the use of substituted pyridine derivatives, which can be complex in the context of future SABRE biomedical applications.<sup>[5]</sup>

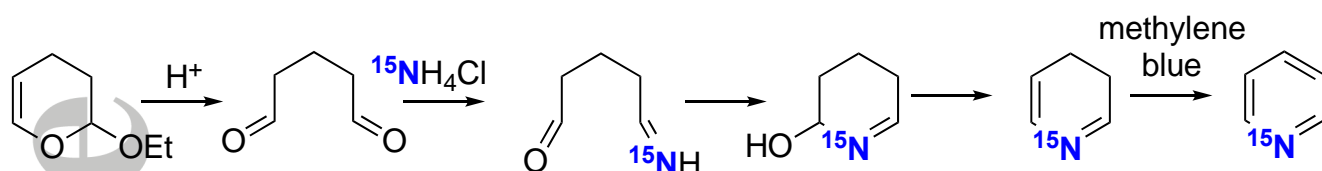


**Figure 3.** Reaction scheme from the previous report<sup>[83]</sup> of <sup>15</sup>N-pyridine synthesis.

An alternative synthetic approach involves the formation of a Zincke salt<sup>[77]</sup> and is followed by reaction with <sup>15</sup>NH<sub>4</sub>Cl (as a source of <sup>15</sup>N label) (Figure 4). To date, this approach has only been applied to the synthesis of <sup>15</sup>N-nicotinamide.<sup>[58, 88, 89]</sup> In the first step, the unlabeled pyridine derivative is reacted with dinitrochlorobenzene to form the Zincke salt (Figure 4). Next, <sup>15</sup>NH<sub>4</sub>Cl is used (as a source of <sup>15</sup>N label) to enable heterocycle ring opening, and dinitroaniline is replaced by <sup>15</sup>N-labeled ammonia. After that, the cyclization proceeds, and the labeled <sup>15</sup>N-pyridine derivative is formed, Figure 4. The reactions shown in Figure 3 and Figure 4 clearly indicate that preparation of <sup>15</sup>N-pyridine derivatives would become challenging using method described in Ref. #<sup>[83]</sup> (because a sophisticated precursor would be required), whereas the Zincke-salt-based approach allows for straightforward <sup>15</sup>N-enrichment using non-labeled biomolecule, e.g. nicotinamide (vitamin B3) shown in Figure 4.

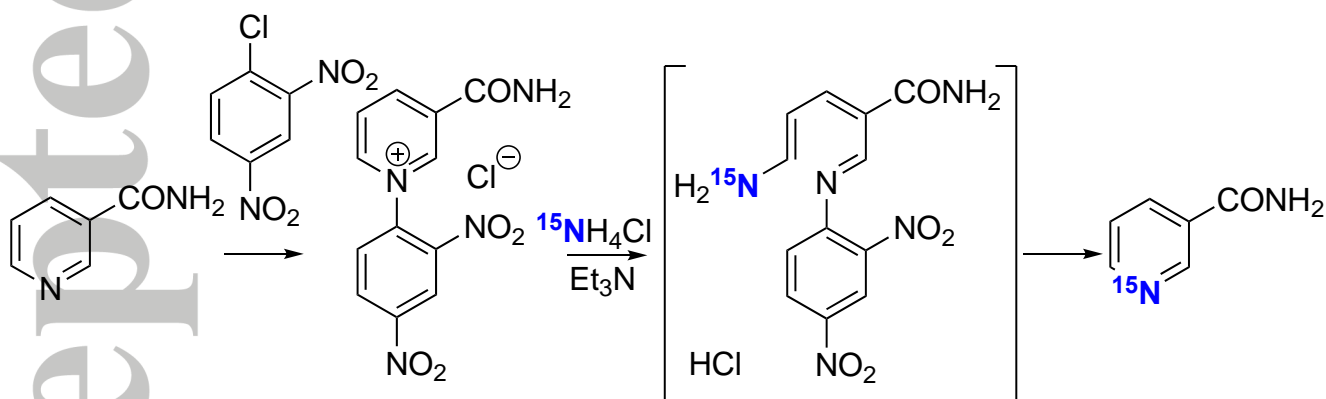


**Figure 4.** Reaction scheme and mechanism for the preparation of <sup>15</sup>N-nicotinamide via formation of Zincke salt.

The less reactive Zincke salts such as 1-N-(2,4-dinitrobenzene) pyridinium chloride have previously been employed to perform ring closure effectively and eliminate the dinitroaniline.<sup>[90]</sup> Therefore, we have employed and investigated this strategy for its potential of <sup>15</sup>N labeling of pyridine.

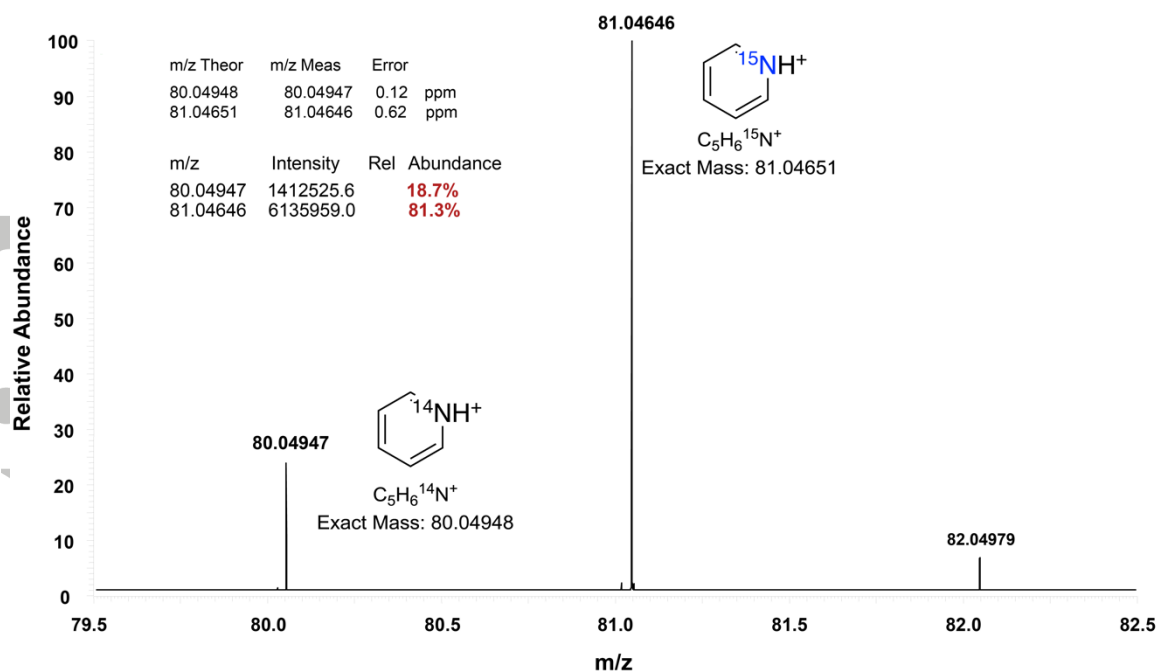


**Figure 5.** High-resolution mass spectrometry of the final product ( $^{15}\text{N}$ -Py) performed by direct liquid infusion using an Orbitrap mass spectrometer (Thermo-Finnigan, San Jose, CA) equipped with an Ion-Max source housing and an atmospheric pressure chemical ionization (APCI) probe in positive ion mode at a resolving power of 60,000 (at  $m/z$  400). Note the presence of the peak at ca. 82.05 due to contribution from  $^{13}\text{C}$  natural abundance of  $\sim 1.1\%$  (therefore, the probability of having one  $^{13}\text{C}$  in any of the five carbon positions is greater than 5%).

An initial quantity of N-(2,4-dinitrophenyl) pyridinium chloride was prepared by interaction of pyridine with 1-chloro-2,4-dinitrobenzene in acetone.<sup>[86]</sup> This salt was used in the reaction with a methanol solution of  $^{15}\text{NH}_4\text{Cl}$  (Figure 2). Purification via filtration with charcoal and the distilling of all volatile compounds including  $^{15}\text{N}$ -Py was performed under atmospheric pressure. We assumed that the slight decomposition of pyridine-Zincke salt back to the unlabeled pyridine during the synthesis and extraction could be responsible for the less-than-ideal isotopic purity at this stage (*i.e.*  $\sim 81\%$  vs. theoretical 98%). Next, the product was extracted in the form of solid pyridinium hydrochloride, which is neutralized by NaOH, and distilled. The final product of  $^{15}\text{N}$ -Py was formed as an aqueous solution with  $\sim 81\%$   $^{15}\text{N}$  isotopic purity confirmed by mass spectrometry analysis, Figures 5.  $^1\text{H}$ ,  $^{13}\text{C}$ , and  $^{15}\text{N}$  NMR spectra are provided in the Supporting Information (Figures S1-S3).

While this  $^{15}\text{N}$  labeling efficiency is lower than that reported by  $^{15}\text{N}$ -nicotinamide (98%), it is relatively high and certainly useful for future biomedical applications of  $^{15}\text{N}$

SABRE hyperpolarization. Of note, pyridine is one of the most studied molecules for the observation of the hyperpolarized  $^1\text{H}$  and  $^{15}\text{N}$  NMR resonances via polarization transfer from parahydrogen via SABRE hyperpolarization approaches, and as a result, this work would be also of interest to those working in the field of fundamental advances of SABRE hyperpolarization technology as well. Moreover, demonstration that the presented approach works for preparation of  $^{15}\text{N}$ -Py (in addition to the previously reported  $^{15}\text{N}$ -nicotinamide preparation<sup>[58]</sup>) opens the road for future  $^{15}\text{N}$ -enrichment of more-complex pyridine derivatives using this relatively straightforward approach. The key synthetic results and their comparison with method described in Ref. #<sup>[83]</sup> are provided in Table 1.

**Table 1. The summary of  $^{15}\text{N}$  pyridine synthesis using presented here method and method employed in Ref. #<sup>[83]</sup>**

	Method from Ref. # <sup>[83]</sup>	This work using Zincke-salt-based method
Reaction Yield	~55%	~33%
$^{15}\text{N}$ isotopic purity	~98%	~81%
Straightforward applicability to preparation of substituted $^{15}\text{N}$ -pyridines	No	Yes

Here, the feasibility of  $^{15}\text{N}$  high-field (HF) SABRE was investigated in the context of an HP MRI application. In the case of HF-SABRE,  $\text{pH}_2$  bubbling through a water-methanol solution of pyridine and homogeneous SABRE catalyst occurred directly inside the high field of a 300 MHz NMR spectrometer along with the recording of  $^{15}\text{N}$  NMR spectra (Figure 6). Under these conditions, the  $^{15}\text{N}$  signal enhancement of the free py resonance is negligible, Figure 6b. The observable HP  $^{15}\text{N}$  NMR signal of the bound  $^{15}\text{N}$ -Py was detected only after 100 averages (~50 seconds of total experimental time). The  $^{15}\text{N}$  signal enhancement factor ( $\epsilon_{^{15}\text{N}}$ ) of *ca.* 100-fold was estimated by comparison of the HP spectrum (Figure 6b) and a thermally polarized spectrum of a  $^{15}\text{N}$  reference sample with known  $^{15}\text{N}$  concentration and polarization (Figure 6a).  $^{15}\text{N}$  SABRE-SHEATH approach (wherein  $\text{pH}_2$  bubbling occurs at a  $\mu\text{T}$  magnetic field created by the magnetic shield followed by fast sample transfer to the high magnetic field for analysis<sup>[56, 57]</sup>) allowed detection of both free and catalyst-bounded  $^{15}\text{N}$ -Py resonances, Figure 6c. As with the case of the HF-SABRE approach the signal enhancement

$\epsilon_{15\text{N}}$  (of approximately about 700-fold) was estimated via comparison of the  $^{15}\text{N}$  HP pyridine resonances with the  $^{15}\text{N}$  signal reference provided by the thermal signal of  $^{15}\text{NH}_4\text{Cl}$  (37%) aqueous solution, Figure 6a, -- in line with previous studies at such concentrations.<sup>[56, 57]</sup>

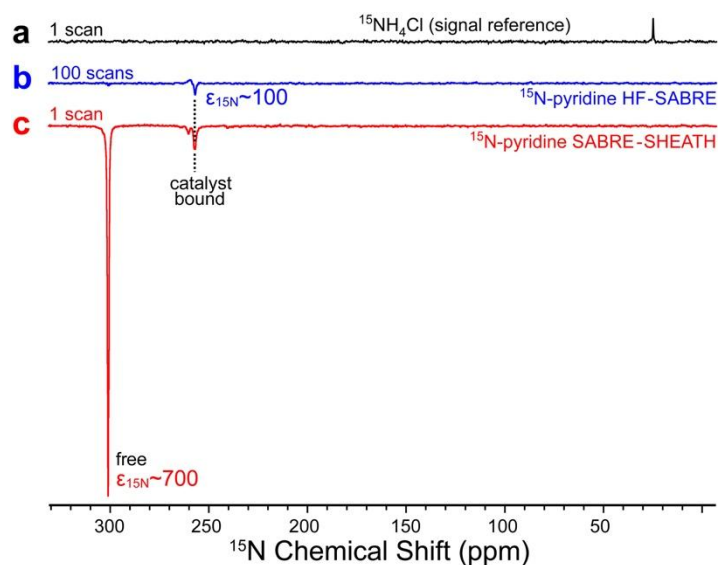


**Figure 6.**  $^{15}\text{N}$  NMR spectra obtained for (a)  $^{15}\text{N}$  signal reference of  $^{15}\text{NH}_4\text{Cl}$  (37%) aqueous solution, (b) HF-SABRE, and (c) SABRE-SHEATH of HP  $^{15}\text{N}$  resonances of  $^{15}\text{N}$ -Py.

While  $^{15}\text{N}$  MRI of SABRE-SHEATH has been demonstrated before,<sup>[57]</sup>  $^{15}\text{N}$  MRI of HF-SABRE has not been investigated. Therefore, the HF-SABRE polarization approach was used to enable  $^{15}\text{N}$  MRI of  $^{15}\text{N}$ -Py. The EPI MRI pulse sequence was employed, and the corresponding  $^{15}\text{N}$  2D MRI image of the cross-section of the 10 mm NMR tube is shown in Figure 7. The imaging spatial resolution was  $2.4 \times 2.4 \text{ mm}^2$ , which is similar to previous resolution ( $2 \times 2 \text{ mm}^2$ ) reported for  $^{15}\text{N}$  SABRE-SHEATH imaging. However, we note that the HF-SABRE MRI image here was recorded at  $\sim 10$  times lower concentration of the HP substrate (i.e., catalyst bound  $^{15}\text{N}$ -Py) and significantly lower (by at least one order of magnitude)  $^{15}\text{N}$  polarization value of the HP  $^{15}\text{N}$ -Py.  $^{15}\text{N}$  MRI with similar spatial resolution (despite nominally lower concentration and nuclear spin polarization) is possible, because  $^{15}\text{N}$  polarization is continuously replenished by the HF-SABRE procedure.

The feasibility of HF-SABRE imaging is important in the context of potential biomedical applications as a facile approach for preparation of HP phantoms to optimize imaging protocols and studies. Moreover, SABRE-SHEATH primarily hyperpolarizes the free  $^{15}\text{N}$  pool (Figure 6c), and therefore MRI imaging of SABRE-SHEATH hyperpolarized solutions reports on spatial distribution of the free pool of HP  $^{15}\text{N}$ -Py. On the other hand, HF-SABRE enhances primarily catalyst-bound species (Figure 6b), and therefore MRI imaging

of HF-SABRE hyperpolarized solutions provides visualization of the catalyst-bound HP  $^{15}\text{N}$ -Py species. Moreover, since HF-SABRE hyperpolarization is quickly replenishable due to continuous  $\text{pH}_2$  bubbling, the additional sensitivity boost due to continuous re-hyperpolarization is achieved, which is advantageous for catalysis visualization via MRI imaging.

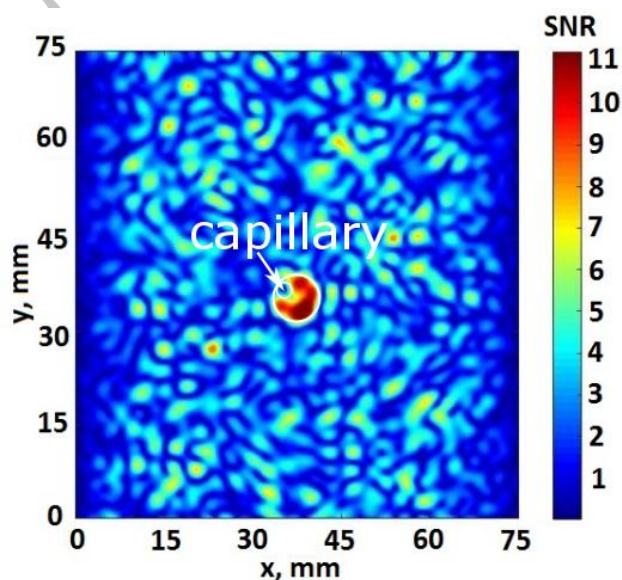


**Figure 7.**  $^{15}\text{N}$  MRI image of high-field (HF)  $^{15}\text{N}$  SABRE of HP  $^{15}\text{N}$ -pyridine obtained using an EPI pulse sequence with 11 ms echo time (TE),  $32 \times 32$  matrix size ( $2.4 \times 2.4 \text{ mm}^2$  pixel size) over  $75 \times 75 \text{ mm}^2$  field of view (FOV), and 4 acquisitions (total experimental time was approximately 4 seconds).

### Conclusions

In summary, an efficient approach for  $^{15}\text{N}$  labeling of pyridine is reported based on the formation of a Zincke salt intermediate. We demonstrated a relatively simple and cheap (1 g of  $^{15}\text{NH}_4\text{Cl}$  costs less than \$20 *ca.* 2017) synthetic approach for the  $^{15}\text{N}$ -enriched pyridine synthesis, which can be used as a robust sample for both SABRE catalyst testing and MRI pulse sequence optimization and other applications. We envision that the relative simplicity and high labeling efficiency (>81%) and overall good yield (>33%) will be of use for future synthetic efforts of labeling of more complex pyridine derivatives in the context of SABRE hyperpolarization and bio-imaging applications. The presented approach is versatile, because it employs the exact non-enriched compound of interest as a precursor in non- $^{15}\text{N}$ -labeled form. Therefore, complex pyridine-based compounds can be  $^{15}\text{N}$ -enriched using this approach. For example, we have recently reported on synthesis of substituted  $^{15}\text{N}$ -pyridine using the reported here approach for preparation of the corresponding Zincke salt.<sup>[91]</sup> The

prepared  $^{15}\text{N}$ -Py was employed for NMR signal hyperpolarization via SABRE technique with signal enhancement of  $^{15}\text{N}$  free resonance of  $\sim 700$ -fold via the SABRE-SHEATH approach and  $^{15}\text{N}$  catalyst-bound resonance of  $\sim 100$ -fold via the HF-SABRE approach.

### Acknowledgements

The Russian team thanks the Russian Science Foundation (grant #17-73-20030) for the support of  $^{15}\text{N}$  pyridine testing via NMR and MRI. N.V.C. thanks Dr. A. I. Taratayko for the useful discussions. This work was supported by NSF under grants CHE-1416268, and CHE-1416432, NIH 1R21EB018014, 1R21EB020323, and 1R21CA220137, DOD CDMRP BRP W81XWH-12-1-0159/BC112431, DOD PRMRP awards W81XWH-15-1-0271 and W81XWH-15-1-0272, and Exxon Mobil Knowledge Build.

### Conflict of Interest

The authors did not report any conflict of interest.

### Corresponding Authors

\*For K.V.K e-mail, [kovtunov@tomo.nsc.ru](mailto:kovtunov@tomo.nsc.ru)

\*For E.Y.C.: phone, +1-(313) 577-2182; fax, +1-(313) 577-8822; e-mail, [chekmenev@wayne.edu](mailto:chekmenev@wayne.edu)

### References

- [1] H. Hiroaki, *Expert Opinion on Drug Discovery* **2013**, *8*, 523.
- [2] J. Kurhanewicz, D. B. Vigneron, K. Brindle, E. Y. Chekmenev, A. Comment, C. H. Cunningham, R. J. DeBerardinis, G. G. Green, M. O. Leach, S. S. Rajan, R. R. Rizi, B. D. Ross, W. S. Warren, C. R. Malloy, *Neoplasia* **2011**, *13*, 81.
- [3] C. S. Clendinen, G. S. Stupp, R. Ajredini, B. Lee-McMullen, C. Beecher, A. S. Edison, *Front. Plant. Sci.* **2015**, *6*, 611.
- [4] V. Theodorou, K. Skobridis, D. Alivertis, I. P. Gerothanassis, *J. Labelled Comp. Radiopharm.* **2014**, *57*, 481.
- [5] P. Nikolaou, B. M. Goodson, E. Y. Chekmenev, *Chem. Eur. J.* **2015**, *21*, 3156.
- [6] B. M. Goodson, N. Whiting, A. M. Coffey, P. Nikolaou, F. Shi, B. M. Gust, M. E. Gemeinhardt, R. V. Shchepin, J. G. Skinner, J. R. Birchall, M. J. Barlow, E. Y. Chekmenev, *Emagres* **2015**, *4*, 797.

- [7] D. A. Barskiy, A. M. Coffey, P. Nikolaou, D. M. Mikhaylov, B. M. Goodson, R. T. Branca, G. J. Lu, M. G. Shapiro, V.-V. Telkki, V. V. Zhivonitko, I. V. Koptug, O. G. Salnikov, K. V. Kovtunov, V. I. Bukhtiyarov, M. S. Rosen, M. J. Barlow, S. Safavi, I. P. Hall, L. Schröder, E. Y. Chekmenev, *Chem. Eur. J.* **2017**, *23*, 725.
- [8] J.-H. Ardenkjaer-Larsen, G. S. Boebinger, A. Comment, S. Duckett, A. S. Edison, F. Engelke, C. Griesinger, R. G. Griffin, C. Hilty, H. Maeda, G. Parigi, T. Prisner, E. Ravera, J. van Bentum, S. Vega, A. Webb, C. Luchinat, H. Schwalbe, L. Frydman, *Angew. Chem. Int. Ed.* **2015**, *54*, 9162.
- [9] S. J. Nelson, J. Kurhanewicz, D. B. Vigneron, P. E. Z. Larson, A. L. Harzstark, M. Ferrone, M. van Criekinge, J. W. Chang, R. Bok, I. Park, G. Reed, L. Carvajal, E. J. Small, P. Munster, V. K. Weinberg, J. H. Ardenkjaer-Larsen, A. P. Chen, R. E. Hurd, L. I. Odegardstuen, F. J. Robb, J. Tropp, J. A. Murray, *Sci. Transl. Med.* **2013**, *5*, 198ra108.
- [10] B. M. Goodson, *J. Magn. Reson.* **2002**, *155*, 157.
- [11] Y. F. Yen, S. J. Kohler, A. P. Chen, J. Tropp, R. Bok, J. Wolber, M. J. Albers, K. A. Gram, M. L. Zierhut, I. Park, V. Zhang, S. Hu, S. J. Nelson, D. B. Vigneron, J. Kurhanewicz, H. Dirven, R. E. Hurd, *Magn. Reson. Med.* **2009**, *62*, 1.
- [12] R. Sriram, J. Kurhanewicz, D. B. Vigneron, in *eMagRes*, John Wiley & Sons, Ltd, **2014**, pp. 311.
- [13] K. V. Kovtunov, A. S. Romanov, O. G. Salnikov, D. A. Barskiy, E. Y. Chekmenev, I. V. Koptug, *Tomography* **2016**, *2*, 49.
- [14] D. B. Burueva, A. S. Romanov, O. G. Salnikov, V. V. Zhivonitko, Y.-W. Chen, D. A. Barskiy, E. Y. Chekmenev, D. W.-H. Hwang, K. V. Kovtunov, I. V. Koptug, *J. Phys. Chem. C* **2017**, *121*, 4481.
- [15] K. V. Kovtunov, M. L. Truong, D. A. Barskiy, I. V. Koptug, A. M. Coffey, K. W. Waddell, E. Y. Chekmenev, *Chem. Eur. J.* **2014**, *20*, 14629.
- [16] K. V. Kovtunov, M. L. Truong, D. A. Barskiy, O. G. Salnikov, V. I. Bukhtiyarov, A. M. Coffey, K. W. Waddell, I. V. Koptug, E. Y. Chekmenev, *J. Phys. Chem. C* **2014**, *118*, 28234.
- [17] D. A. Barskiy, O. G. Salnikov, A. S. Romanov, M. A. Feldman, A. M. Coffey, K. V. Kovtunov, I. V. Koptug, E. Y. Chekmenev, *J. Magn. Reson.* **2017**, *276*, 78.
- [18] D. A. Barskiy, O. G. Salnikov, R. V. Shchepin, M. A. Feldman, A. M. Coffey, K. V. Kovtunov, I. V. Koptug, E. Y. Chekmenev, *J. Phys. Chem. C* **2016**, *120*, 29098.
- [19] E. R. McCarney, B. D. Armstrong, M. D. Lingwood, S. Han, *Proc. Natl. Acad. Sci. U. S. A.* **2007**, *104*, 1754.
- [20] A. M. Coffey, K. V. Kovtunov, D. Barskiy, I. V. Koptug, R. V. Shchepin, K. W. Waddell, P. He, K. A. Groome, Q. A. Best, F. Shi, B. M. Goodson, E. Y. Chekmenev, *Anal. Chem.* **2014**, *86*, 9042.
- [21] O. G. Salnikov, D. A. Barskiy, A. M. Coffey, K. V. Kovtunov, I. V. Koptug, E. Y. Chekmenev, *ChemPhysChem* **2016**, *17*, 3395.
- [22] Y. Zhang, X. Duan, P. C. Soon, V. Sychrovský, J. W. Canary, A. Jerschow, *ChemPhysChem* **2016**, *17*, 2967.
- [23] K. Golman, R. in't Zandt, M. Thaning, *Proc. Natl. Acad. Sci. U. S. A.* **2006**, *103*, 11270.
- [24] S. E. Day, M. I. Kettunen, F. A. Gallagher, D. E. Hu, M. Lerche, J. Wolber, K. Golman, J. H. Ardenkjaer-Larsen, K. M. Brindle, *Nat. Med.* **2007**, *13*, 1382.
- [25] K. Golman, O. Axelsson, H. Johannesson, S. Mansson, C. Olofsson, J. S. Petersson, *Magn. Reson. Med.* **2001**, *46*, 1.
- [26] P. Bhattacharya, E. Y. Chekmenev, W. H. Perman, K. C. Harris, A. P. Lin, V. A. Norton, C. T. Tan, B. D. Ross, D. P. Weitekamp, *J. Magn. Reson.* **2007**, *186*, 150.

- [27] P. Bhattacharya, E. Y. Chekmenev, W. F. Reynolds, S. Wagner, N. Zacharias, H. R. Chan, R. Bünger, B. D. Ross, *NMR Biomed.* **2011**, *24*, 1023.
- [28] A. M. Coffey, R. V. Shchepin, M. L. Truong, K. Wilkens, W. Pham, E. Y. Chekmenev, *Anal. Chem.* **2016**, *88*, 8279.
- [29] A. M. Coffey, M. A. Feldman, R. V. Shchepin, D. A. Barskiy, M. L. Truong, W. Pham, E. Y. Chekmenev, *J. Magn. Reson.* **2017**, *281*, 246.
- [30] M. Durst, E. Chiavazza, A. Haase, S. Aime, M. Schwaiger, R. F. Schulte, *Magn. Reson. Med.* **2016**, *76*, 1900.
- [31] C. Cudalbu, A. Comment, F. Kurdzesau, R. B. van Heeswijk, K. Uffmann, S. Jannin, V. Denisov, D. Kirik, R. Gruetter, *Phys. Chem. Chem. Phys.* **2010**, *12*, 5818.
- [32] C. Gabellieri, S. Reynolds, A. Lavie, G. S. Payne, M. O. Leach, T. R. Eykyn, *J. Am. Chem. Soc.* **2008**, *130*, 4598.
- [33] L. Bales, K. V. Kovtunov, D. A. Barskiy, R. V. Shchepin, A. M. Coffey, L. M. Kovtunova, A. V. Bukhtiyarov, M. A. Feldman, V. I. Bukhtiyarov, E. Y. Chekmenev, I. V. Koptug, B. M. Goodson, *J. Phys. Chem. C* **2017**, *121*, 15304.
- [34] K. V. Kovtunov, L. M. Kovtunova, M. E. Gemeinhardt, A. V. Bukhtiyarov, J. Gesiorski, V. I. Bukhtiyarov, E. Y. Chekmenev, I. V. Koptug, B. M. Goodson, *Angew. Chem. Int. Ed.* **2017**, *56*, 10433.
- [35] K. V. Kovtunov, D. A. Barskiy, O. G. Salnikov, R. V. Shchepin, A. M. Coffey, L. M. Kovtunova, V. I. Bukhtiyarov, I. V. Koptug, E. Y. Chekmenev, *RSC Adv.* **2016**, *6*, 69728.
- [36] K. V. Kovtunov, D. A. Barskiy, R. V. Shchepin, O. G. Salnikov, I. P. Prosvirin, A. V. Bukhtiyarov, L. M. Kovtunova, V. I. Bukhtiyarov, I. V. Koptug, E. Y. Chekmenev, *Chem. Eur. J.* **2016**, *22*, 16446.
- [37] R. Hata, H. Nonaka, Y. Takakusagi, K. Ichikawa, S. Sando, *Chem. Comm.* **2015**, *51*, 12290.
- [38] H. Nonaka, M. Hirano, Y. Imakura, Y. Takakusagi, K. Ichikawa, S. Sando, *Sci. Rep.* **2017**, *7*, 40104.
- [39] R. Sarkar, A. Comment, P. R. Vasos, S. Jannin, R. Gruetter, G. Bodenhausen, H. Hall, D. Kirik, V. P. Denisov, *J. Am. Chem. Soc.* **2009**, *131*, 16014.
- [40] T. Theis, G. X. Ortiz, A. W. J. Logan, K. E. Claytor, Y. Feng, W. P. Huhn, V. Blum, S. J. Malcolmson, E. Y. Chekmenev, Q. Wang, W. S. Warren, *Sci. Adv.* **2016**, *2*, e1501438.
- [41] M. J. Albers, R. Bok, A. P. Chen, C. H. Cunningham, M. L. Zierhut, V. Y. Zhang, S. J. Kohler, J. Tropp, R. E. Hurd, Y.-F. Yen, S. J. Nelson, D. B. Vigneron, J. Kurhanewicz, *Cancer Res.* **2008**, *68*, 8607.
- [42] P. E. Z. Larson, S. Hu, M. Lustig, A. B. Kerr, S. J. Nelson, J. Kurhanewicz, J. M. Pauly, D. B. Vigneron, *Magn. Reson. Med.* **2011**, *65*, 610.
- [43] W. Jiang, L. Lumata, W. Chen, S. Zhang, Z. Kovacs, A. D. Sherry, C. Khemtong, *Sci. Rep.* **2015**, *5*, 9104.
- [44] J. H. Ardenkjaer-Larsen, B. Fridlund, A. Gram, G. Hansson, L. Hansson, M. H. Lerche, R. Servin, M. Thaning, K. Golman, *Proc. Natl. Acad. Sci. U. S. A.* **2003**, *100*, 10158.
- [45] F. Reineri, A. Viale, S. Ellena, D. Alberti, T. Boi, G. B. Giovenzana, R. Gobetto, S. S. D. Premkumar, S. Aime, *J. Am. Chem. Soc.* **2012**, *134*, 11146.
- [46] M. Carravetta, O. G. Johannessen, M. H. Levitt, *Phys. Rev. Lett.* **2004**, *92*, 153003.
- [47] R. V. Shchepin, D. A. Barskiy, A. M. Coffey, T. Theis, F. Shi, W. S. Warren, B. M. Goodson, E. Y. Chekmenev, *ACS Sensors* **2016**, *1*, 640.

- [48] R. W. Adams, J. A. Aguilar, K. D. Atkinson, M. J. Cowley, P. I. P. Elliott, S. B. Duckett, G. G. R. Green, I. G. Khazal, J. Lopez-Serrano, D. C. Williamson, *Science* **2009**, *323*, 1708.
- [49] R. W. Adams, S. B. Duckett, R. A. Green, D. C. Williamson, G. G. R. Green, *J. Chem. Phys.* **2009**, *131*, 194505.
- [50] K. V. Kovtunov, I. E. Beck, V. V. Zhivonitko, D. A. Barskiy, V. I. Bukhtiyarov, I. V. Koptuyug, *Phys. Chem. Chem. Phys.* **2012**, *14*, 11008.
- [51] K. V. Kovtunov, V. V. Zhivonitko, I. V. Skovpin, D. A. Barskiy, O. G. Salnikov, I. V. Koptuyug, *J. Phys. Chem. C* **2013**, *117*, 22887.
- [52] D. A. Barskiy, R. V. Shchepin, A. M. Coffey, T. Theis, W. S. Warren, B. M. Goodson, E. Y. Chekmenev, *J. Am. Chem. Soc.* **2016**, *138*, 8080.
- [53] J. F. P. Colell, A. W. J. Logan, Z. Zhou, R. V. Shchepin, D. A. Barskiy, G. X. Ortiz, Q. Wang, S. J. Malcolmson, E. Y. Chekmenev, W. S. Warren, T. Theis, *J. Phys. Chem. C* **2017**, *121*, 6626.
- [54] J. F. P. Colell, M. Emondts, A. W. J. Logan, K. Shen, J. Bae, R. V. Shchepin, G. X. Ortiz, P. Spanring, Q. Wang, S. J. Malcolmson, E. Y. Chekmenev, M. C. Feiters, F. P. J. T. Rutjes, B. Bluemich, T. Theis, W. S. Warren, *J. Am. Chem. Soc.* **2017**, *139*, 7761.
- [55] A. W. J. Logan, T. Theis, J. F. P. Colell, W. S. Warren, S. J. Malcolmson, *Chem. Eur. J.* **2016**, *22*, 10777.
- [56] T. Theis, M. L. Truong, A. M. Coffey, R. V. Shchepin, K. W. Waddell, F. Shi, B. M. Goodson, W. S. Warren, E. Y. Chekmenev, *J. Am. Chem. Soc.* **2015**, *137*, 1404.
- [57] M. L. Truong, T. Theis, A. M. Coffey, R. V. Shchepin, K. W. Waddell, F. Shi, B. M. Goodson, W. S. Warren, E. Y. Chekmenev, *J. Phys. Chem. C* **2015**, *119*, 8786.
- [58] R. V. Shchepin, D. A. Barskiy, D. M. Mikhaylov, E. Y. Chekmenev, *Bioconjugate Chem.* **2016**, *27*, 878.
- [59] R. V. Shchepin, D. A. Barskiy, A. M. Coffey, M. A. Feldman, L. M. Kovtunova, V. I. Bukhtiyarov, K. V. Kovtunov, B. M. Goodson, I. V. Koptuyug, E. Y. Chekmenev, *ChemistrySelect* **2017**, *2*, 4478.
- [60] R. V. Shchepin, E. Y. Chekmenev, *J. Labelled Comp. Radiopharm.* **2014**, *57*, 621.
- [61] K. T. Neumann, A. T. Lindhardt, B. Bang-Andersen, T. Skrydstrup, *J. Labelled Comp. Radiopharm.* **2017**, *60*, 30.
- [62] J. H. Ardenkjaer-Larsen, *J. Magn. Reson.* **2016**, *264*, 3.
- [63] R. E. Mewis, *Magn. Reson. Chem.* **2015**, *53*, 789.
- [64] R. A. Green, R. W. Adams, S. B. Duckett, R. E. Mewis, D. C. Williamson, G. G. R. Green, *Prog. Nucl. Mag. Res. Spectrosc.* **2012**, *67*, 1.
- [65] R. V. Shchepin, D. A. Barskiy, A. M. Coffey, B. M. Goodson, E. Y. Chekmenev, *ChemistrySelect* **2016**, *1*, 2552.
- [66] T. Theis, M. Truong, A. M. Coffey, E. Y. Chekmenev, W. S. Warren, *J. Magn. Reson.* **2014**, *248*, 23.
- [67] A. N. Pravdivtsev, A. V. Yurkovskaya, H. Zimmermann, H.-M. Vieth, K. L. Ivanov, *RSC Adv.* **2015**, *5*, 63615.
- [68] V. V. Zhivonitko, I. V. Skovpin, I. V. Koptuyug, *Chem. Comm.* **2015**, *51*, 2506.
- [69] D. A. Barskiy, R. V. Shchepin, C. P. N. Tanner, J. F. P. Colell, B. M. Goodson, T. Theis, W. S. Warren, E. Y. Chekmenev, *ChemPhysChem* **2017**, *18*, 1493.
- [70] Z. Zhou, J. Yu, J. F. P. Colell, R. Laasner, A. W. J. Logan, D. A. Barskiy, R. V. Shchepin, E. Y. Chekmenev, V. Blum, W. S. Warren, T. Theis, *J. Phys. Chem. Lett.* **2017**, *8*, 3008.
- [71] R. V. Shchepin, B. M. Goodson, T. Theis, W. S. Warren, E. Y. Chekmenev, *ChemPhysChem* **2017**, *18*, 1961.

- [72] A. M. Olaru, A. Burt, P. J. Rayner, S. J. Hart, A. C. Whitwood, G. G. R. Green, S. B. Duckett, *Chem. Comm.* **2016**, 52, 14482.
- [73] K. D. Atkinson, M. J. Cowley, S. B. Duckett, P. I. P. Elliott, G. G. R. Green, J. López-Serrano, I. G. Khazal, A. C. Whitwood, *Inorg. Chem.* **2009**, 48, 663.
- [74] K. D. Atkinson, M. J. Cowley, P. I. P. Elliott, S. B. Duckett, G. G. R. Green, J. Lopez-Serrano, A. C. Whitwood, *J. Am. Chem. Soc.* **2009**, 131, 13362.
- [75] M. J. Cowley, R. W. Adams, K. D. Atkinson, M. C. R. Cockett, S. B. Duckett, G. G. R. Green, J. A. B. Lohman, R. Kerssebaum, D. Kilgour, R. E. Mewis, *J. Am. Chem. Soc.* **2011**, 133, 6134.
- [76] R. V. Shchepin, M. L. Truong, T. Theis, A. M. Coffey, F. Shi, K. W. Waddell, W. S. Warren, B. M. Goodson, E. Y. Chekmenev, *J. Phys. Chem. Lett.* **2015**, 6, 1961.
- [77] T. Zincke, G. Heuser, W. Möller, *Justus Liebigs Ann. Chem.* **1904**, 333, 296.
- [78] D. A. Barskiy, K. V. Kovtunov, I. V. Koptug, P. He, K. A. Groome, Q. A. Best, F. Shi, B. M. Goodson, R. V. Shchepin, M. L. Truong, A. M. Coffey, K. W. Waddell, E. Y. Chekmenev, *ChemPhysChem* **2014**, 15, 4100.
- [79] K. L. Ivanov, A. N. Pravdivtsev, A. V. Yurkovskaya, H.-M. Vieth, R. Kaptein, *Prog. Nucl. Mag. Res. Spectrosc.* **2014**, 81, 1.
- [80] S. Knecht, A. N. Pravdivtsev, J.-B. Hovener, A. V. Yurkovskaya, K. L. Ivanov, *RSC Adv.* **2016**, 6, 24470.
- [81] A. N. Pravdivtsev, A. V. Yurkovskaya, P. A. Petrov, H.-M. Vieth, K. L. Ivanov, *Appl. Magn. Reson.* **2016**, 47, 711.
- [82] M. L. Truong, F. Shi, P. He, B. Yuan, K. N. Plunkett, A. M. Coffey, R. V. Shchepin, D. A. Barskiy, K. V. Kovtunov, I. V. Koptug, K. W. Waddell, B. M. Goodson, E. Y. Chekmenev, *J. Phys. Chem. B* **2014**, 18, 13882.
- [83] T. W. Whaley, D. G. Ott, *J. Labelled Comp.* **1974**, 10, 283.
- [84] J.-B. Hövener, A. N. Pravdivtsev, B. Kidd, C. R. Bowers, S. Glögler, K. V. Kovtunov, M. Plaumann, R. Katz-Brull, K. Buckenmaier, A. Jerschow, F. Reineri, T. Theis, R. V. Shchepin, S. Wagner, P. Bhattacharya, N. M. Zacharias, E. Y. Chekmenev, *Angew. Chem. Int. Ed.* **2018**, 57, 11140.
- [85] D. A. Barskiy, K. V. Kovtunov, I. V. Koptug, P. He, K. A. Groome, Q. A. Best, F. Shi, B. M. Goodson, R. V. Shchepin, A. M. Coffey, K. W. Waddell, E. Y. Chekmenev, *J. Am. Chem. Soc.* **2014**, 136, 3322.
- [86] O. A. Okoh, R. H. Bisby, C. L. Lawrence, C. E. Rolph, R. B. Smith, *J. Sulfur Chem.* **2014**, 35, 42.
- [87] L. D. Vazquez-Serrano, B. T. Owens, J. M. Buriak, *Inorg. Chim. Acta* **2006**, 359, 2786.
- [88] N. J. Oppenheimer, T. O. Matsunaga, B. L. Kam, *J. Labelled Comp. Radiopharm.* **1978**, 15, 191.
- [89] E. S. Burgos, M. J. Veticatt, V. L. Schramm, *J. Am. Chem. Soc.* **2013**, 135, 3485.
- [90] M. R. Atkinson, R. K. Morton, R. Naylor, *J. Chem. Soc.* **1965**, 610.
- [91] N. V. Chukanov, O. G. Salnikov, R. V. Shchepin, A. Svyatova, K. V. Kovtunov, I. V. Koptug, E. Y. Chekmenev, *J. Phys. Chem. C* **2018**, 122, 23002.